Quantum Dot-Cavity Coupling with Phonon-Assisted Cavity Feeding

Georg Wissa

2010

Contents

Chapter 1

Introduction

A quantum dot can trap an exciton.
An exciton can decay into a photon.
A photon can be trapped in a micro-cavity.
A quantum dot coupled to a suitable micro-cavity can lead to new properties.

Quantum Dots (QDs) are an exciting tool to investigate experimentally quantum mechanic theory, and promise applications as ultra low threshold lasers and single photon sources.

This work focuses on solid-state QDs, consisting of semiconductor materials (e.g. GaAs/InAs QD). In such QDs it is possible to confine electron-hole-pairs, which interact via the Coulomb potential, so called excitons. As these confined excitons posses discrete bound states (discrete energy-levels), they are often named "artificial-atoms". However, in contrast to single atoms the QDs are embedded in a solid host matrix. This allows for an additional non-radiative interaction, namely the absorption of a phonon or opens new interaction channels, such as the emission of phonons or coupling with the nuclear spins.

Embedding the QD in a suitable cavity allows to form a coupled system. When the frequency of the QD transition (ω_{qd}) and the cavity frequency (ω_{cav}) are tuned close to resonance: Several phenomena can be observed; dressed state form, single charges or spin excitations can be optically controlled. This can be used for ultra low threshold nanolasers or controll of the spontaneous emission properties of QD emitters (*Purcell effect*).

In the remainder of this chapter some basic information is provided about QDs and photonic crystal cavities. In chapter 2 an introduction to Quantum Dot-Cavity-Coupling will be given in the framework of Cavity-Quantum Electrodynamics described by the **Jaynes-Cummings Model**. The theory is discussed for closed system in chapter 2 and for open system in chapter 3, where dissipative processes with the environment are included. In particular spontaneous emission

with rate γ and cavity leakage mirror with the rate κ are considered. Detuning of the resonance frequency of the cavity with respect to the QD frequency can be compensated by phonon assisted cavity feeding, as is discussed in chapter 4.

1.1 Solid State Quantum Dots

A quantum dot (QD) is a nanoscopic solid state object that possesses atom-like properties. In particular a QD can emit a discrete light spectrum, i.e. photons with well defined energies. The quantization of the energy levels stems from the fact that the dimensions of the QDs are in the same range as the de-Broglie-wavelength

$$\lambda = h/p = \frac{1.22}{E_{kin}} \tag{1.1}$$

of the conduction carriers (electron, hole). For precise description of the energy levels the effective potential of the QD has to be known. This potential depends on material and shape of the QD and, to some extent, also on the temperature.

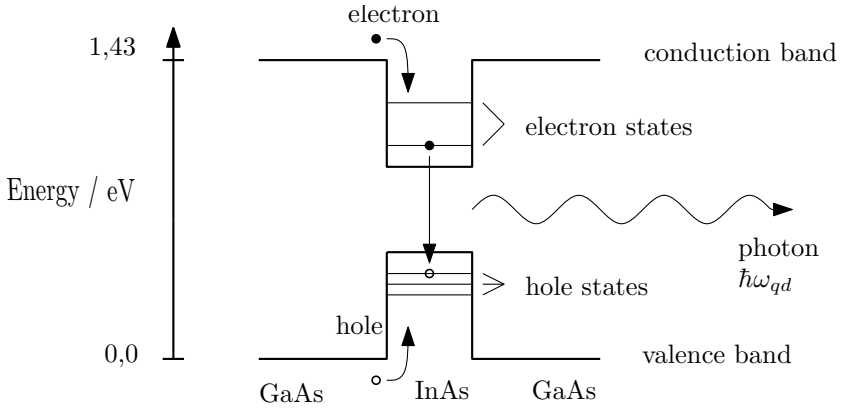

Figure 1.1: Simplified band gap scheme of a InAs quantum dot embedded in GaAs: The confinement potential of the quantum dot leads to discrete energy levels.

QDs consist commonly of semiconducting materials, where the band gap and consequently the energy of absorbed and emitted photons can be chosen by using the appropriate semiconductor materials. A system widely explored in literature [11] are InAs QDs that are embedded in a GaAs host matrix [band gap energies: InAs $\Delta E_g(InAs) = 0.36eV$, GaAs ($\Delta E_g(GaAs) = 1.43eV$]. GaAs is a typical semiconductor, for optoelectronic applications at the telecom frequencies ($1.3\mu m, 1.55\mu m$). Because InAs has a somewhat different lattice constant compared to GaAs, self assembled nanoscopic dots can be produced when a few layers of InAs are deposited onto a GaAs surface, for example by molecular beam epitaxy [11]. The resulting small islands show a lens shaped material distribution (widths and hights a few nm) and exhibit sharp optical transitions [11]. The

growth conditions determine the height and width, and the optical quality of the QDs, and consequently the transition frequency.

An exciton is an electron-hole pair that can be produced, for example, when a photon is absorbed in a semiconductor. There exist rather complicated types of excitons, in particular when the spin of an electron is considered. However, in this work only the simple case of a two level system (exciton present or absent) is examined.

A typical mechanism that causes photon emission in QDs is depicted in figure 1.1. First an exciton is optically excited in the host material. This exciton becomes trapped in the QD. The eventual energy mismatch can be compensated by phonon emission. Here the smaller energy gap of the QD demands phonon emission, causing a local heating of the material. A recombination of electron and hole (decay of the exciton) results in the emission of a photon.

1.2 Photonic Crystal Microcavities

A photonic crystal is formed by a regular arrangement of two materials with different optical refractive indices. This optical grating supports the propagation of electromagnetic waves (light) with certain frequencies ω due to constructive interference, while other frequencies are forbidden (destructive interference). Microscopic optical elements can be obtained when some of the grating elements are missing. For example a line of missing grating elements results in a wave guide, while a single or a few missing elements can act as a resonator (micro-cavity). A photonic crystal cavity centered around a single QD was produced by Hennessey et al. [5], as can be seen in figure 1.2. In this case the QD is centered in the maximum of an optical mode of the cavity, which allows optimum QD-cavity-coupling.

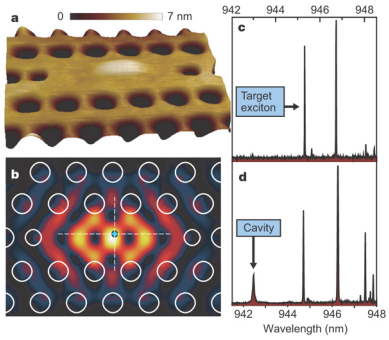

Figure 1.2: AFM-image of a single QD embedded in the center of a photonic crystal micro-cavity (a) and calculated fundamental optical mode of the resonator (b). Taken from [5].

A photonic crystal allows to reduce the losses of excitons trapped in QDs. Furthermore, the photonic band gap allows to manipulate the spontaneous emission of the embedded QDs.

1.3 Coupling of QDs to photonic crystals

When a QD is coupled to a photonic crystal cavity specific properties can be manipulated and new effects arise.

It is difficult to place the QD in the center of a photonic crystal cavity as both the QDs and the photonic crystal have to be produced on a nanoscopic scale. An excellent interaction can be attained when the QD is placed such in the resonator that it is located at the antinode of the fundamental modes of the resonator, as has been shown by [11], see figure 1.2. Another possibility is to choose the density of randomly located QDs such that statistically at least one is located in the cavity of the embedding photonic crystal structure.

Now consider a QD that is located in the cavity of a photonic crystal. When the QD emits a photon with a frequency similar to an optical eigenfrequency of the cavity, the photon can be trapped in the cavity. Then it can again excite an exciton leading again to photon emission in the cavity, etc. (like two coupled pendula with the same eigenfrequenceies).

Chapter 2

Cavity Quantum Electrodynamics: Jaynes Cummings Model

The coupled system of a quantum dot and a micro-cavity can be described by the Jaynes Cummings Model. It allows for a quantum mechanical description of the coupling of the dipole moment of an exciton with a cavity mode.

To describe this system it is necessary to quantize the electromagnetic radiation field. Considering a cavity with fixed boundary conditions, the radiation field can be represented by just one harmonic oscillator mode. If the transition energy of the QD $\hbar\omega_{qd}$ is near resonance with the interacting cavity-mode $\hbar\omega_{cav}$, transitions between other states are negligible and the QD may be idealized as a two-level QD. This idealized picture does not include optical losses of the cavity mode (κ) and spontaneous emission of the QD (γ) into optical modes outside the cavity (continuous vacuum).

In this chapter we start by introducing the description models for QD and cavity. Then we describe the uncoupled system QD-cavity and the coupled QD-cavity system and the resulting emergence of quasi-particles which have partly excitonic and partly cavity character (polaritons).

2.1 Theoretical Model of a Quantum Dot

The quantum dot can be described as an "artificial atom", because it exhibits atom-like discrete energy-levels. The Jaynes Cummings Model considers the quantum dot as a two-level-system (see figure 2.1) with ground-state $|g\rangle$ and excited-state $|e\rangle$. The Hamiltonian of the QD reads

$$\hat{H}_{\mathrm{qd}} = E_g|g\rangle\langle g| + E_e|e\rangle\langle e| = \hbar\omega_{qd}\hat{\sigma}_+\hat{\sigma}_- \,, \tag{2.1}$$

where $\hbar\omega_{qd}$ is the energy gap $\hbar\omega_{qd} = E_e - E_g$ between energy of the ground-state E_g and the excited-state E_e. $\hat{\sigma}_+$ and $\hat{\sigma}_-$ are the excitonic *creation* and *annihilation operators* defined as $\hat{\sigma}_+ \equiv |e\rangle\langle g|$ and $\hat{\sigma}_- \equiv |g\rangle\langle e|$.

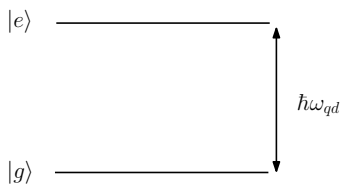

Figure 2.1: Two-level-system of a QD with ground-state $|g\rangle$ and excited-state $|e\rangle$.

2.2 Theoretical Model of a Micro-Cavity

A quantized electromagnetic field can be described in terms of quantum harmonic oscillator modes [2]. In the most simple case the cavity sustains one optical mode, described by one harmonic oscillator, as can be seen in figure 2.2. Its Hamiltonian reads

$$\hat{H} = \hbar\omega_{cav}(\hat{a}^\dagger\hat{a} + \frac{1}{2}), \tag{2.2}$$

with $\hat{a}^\dagger$ and $\hat{a}$ being *creation* and *annihilation operators* which raise or lower the occupation number n of the state of the harmonic oscillator by one photon. Here we neglect the energy of the ground state $\hbar\omega_{cav}/2$, so the Hamiltonian reads

$$\hat{H}_{cav} = \hbar\omega_{cav}\hat{a}^\dagger\hat{a} \tag{2.3}$$

with

$$\hat{H}_{cav}|n\rangle = \hbar\omega_{cav}n|n\rangle \tag{2.4}$$
$$\hat{a}^\dagger|n\rangle = \sqrt{n+1}|n+1\rangle \tag{2.5}$$
$$\hat{a}|n\rangle = \sqrt{n}|n-1\rangle \tag{2.6}$$
$$\hat{a}^\dagger\hat{a}|n\rangle = n|n\rangle, \tag{2.7}$$

where $|n\rangle$ is a Fock-state.

2.3 Uncoupled System: $\hat{H}_{qd} + \hat{H}_{cav}$

When the QD and the cavity are not coupled the Hamiltonian of the system reads

$$\hat{H} = \hat{H}_{qd} + \hat{H}_{cav} = \hbar\omega_{qd}\hat{\sigma}_+\hat{\sigma}_- + \hbar\omega_{cav}\hat{a}^\dagger\hat{a}. \tag{2.8}$$

The global state of the uncoupled system is defined by the tensor product of the two initially individual spaces $\mathcal{H}_{qd}$ and $\mathcal{H}_{cav}$ of the QD and the cavity $\mathcal{H} =$

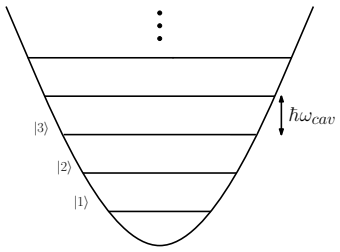

Figure 2.2: Energy levels of a cavity-mode modeled by one harmonic oscillator.

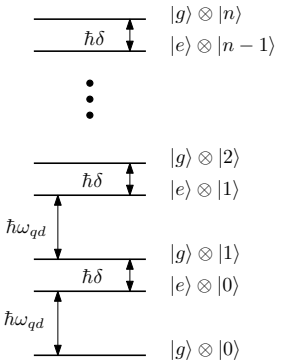

Figure 2.3: Ladder energy scheme for uncoupled QD-cavity-system. Here the energy mismatch $\delta = \omega_{cav} - \omega_{qd} > 0$.

$\mathcal{H}_{qd} \otimes \mathcal{H}_{cav}$, where the pairs $\{|g\rangle \otimes |n\rangle, |e\rangle \otimes |n\rangle\}$ form an orthogonal basis. The eigen-equations for the uncoupled system read

$$H|g\rangle \otimes |n\rangle = \hbar\omega_{cav}|g\rangle \otimes |n\rangle \tag{2.9}$$
$$H|e\rangle \otimes |n\rangle = (\hbar\omega_{qd} + n\hbar\omega_{cav})\,|e\rangle \otimes |n\rangle. \tag{2.10}$$

The corresponding eigen-energies with $\delta = \omega_{cav} - \omega_{qd}$ read

$$E_{g,0} = 0 \tag{2.11}$$
$$E_{g,n} = n\hbar\omega_{cav} \tag{2.12}$$
$$E_{e,n} = \hbar\omega_{qd} + n\hbar\omega_{cav} = (n+1)\hbar\omega_{cav} - \hbar\delta \tag{2.13}$$
$$E_{g,n} - E_{e,n-1} = \hbar\delta, \quad E_{e,n} - E_{g,n} = \hbar\omega_{qd} \tag{2.14}$$

Although the system is uncoupled the QM description yields a new more complex scheme of global energy levels, as can be seen in figure(2.3). This scheme is called an energy ladder consisting of energy levels with two different values of energy spacings ($\hbar\omega_{qd}$ and δ).

2.4 Coupled System: $\hat{H}_{qd} + \hat{H}_{cav} + \hat{H}_{int}$

2.4.1 Coupled System Hamiltonian

QD-cavity interaction can be modeled as the interaction between an electromagnetic (EM) field and an atom. For this coupled system we start with the classical Maxwell-atom-light interaction. Transforming the EM field vectors into QM field operators provides a QM description for the interaction between light and the dipole moment of the atom.

The EM field is represented by the vector potential $\mathbf{A}$ and scalar potential Φ. The Hamiltonian H of an Maxwell-atom-light interaction reads [4]

$$H = \sum_{i=e,h} \left(\frac{1}{2m_i} \left[\hat{\mathbf{p}}_i + (e/c)\mathbf{A}(\mathbf{r}_i, t) \right]^2 - e\Phi(\mathbf{r}_i) \right) + V_{coul} + H_{rad} \,. \tag{2.15}$$

The first term of H (namely$[\hat{\mathbf{p}}_i + (e/c)\mathbf{A}(\mathbf{r}_i, t)]^2$) is the kinetic energy of the particle with m_i the electron/hole mass. The Coulomb energy V_{coul} between electron and hole (exciton) is included in the QM description of the two-level-QD system approximation, as discussed in section 2.1. The third term represents the energy of the (transverse) radiation field H_{rad} [1].

To describe phenomena like spontaneous emission of light from the exciton into the cavity it is necessary to quantize the EM field. The EM potentials have do be replaced by their corresponding quantum mechanical operators $\hat{\mathbf{A}}$. Solving equation (2.15) by using the Coulomb-gauge $\boldsymbol{\nabla}\mathbf{A} = 0$ results in $\Phi = 0$.[2]

The Hamiltonian $\hat{H}$ of the uncoupled QD-cavity system, that corresponds to equation (2.15), can be written as

$$\hat{H} = \hat{H}_0 + \hat{H}_{int} \,, \tag{2.16}$$

with the free Hamiltonian (as defined in section 2.2)

$$\begin{aligned} \hat{H}_0 &= \hat{H}_{qd} + \hat{H}_{cav} \\ &= \hbar\omega_{qd}\hat{\sigma}_+\hat{\sigma}_- + \sum_{\lambda} \hbar\omega_{cav}\hat{a}^\dagger_\lambda \hat{a}_\lambda \,. \end{aligned} \tag{2.17}$$

Where only one cavity-mode is considered in form of a harmonic oscillator with two directions of polarization ($\lambda = 1, 2$). The interaction Hamiltonian reads

$$\hat{H}_{int} = \sum_{i=e,h} \frac{e}{2\mu c} \left(\hat{\mathbf{p}}_i \cdot \hat{\mathbf{A}}(\mathbf{r}_i) + \hat{\mathbf{A}}(\mathbf{r}_i) \cdot \hat{\mathbf{p}}_i \right) + \frac{e^2}{2\mu c^2} \left(\hat{\mathbf{A}}(\mathbf{r}_i) \right)^2 \tag{2.18}$$

[1] $H_{rad} = \frac{\epsilon_0}{2} \int d^3r \left[\mathbf{E}^2_\perp(\mathbf{r}) + c^2\mathbf{B}^2(\mathbf{r}) \right]$ whose corresponding quantum mechanical expression is $\hat{H}_{cav}$ as introduced in section 2.2.

[2] For the radiation field the only independent variables are the transverse vector potential $\mathbf{A}_\perp$ and its velocity $\dot{\mathbf{A}} = -\mathbf{E}_\perp$.

with

$$\hat{\mathbf{A}}(\mathbf{r}) = \sqrt{\frac{2\pi\hbar c^2}{\omega_{cav} L^3}} \sum_{\lambda=1}^{2} \left(\boldsymbol{\pi}_\lambda e^{i\mathbf{k}\cdot\mathbf{r}} \hat{a}_\lambda + \boldsymbol{\pi}_\lambda^* e^{-i\mathbf{k}\cdot\mathbf{r}} \hat{a}_\lambda^\dagger \right) \tag{2.19}$$

being the QM vector potential operator of one mode. $\boldsymbol{\pi}_\lambda$ is the complex polarization vector of the electromagnetic field mode with wave vector $\mathbf{k}$, polarization state λ and frequency ω_{cav}.

Approximations of the interaction Hamiltonian $\hat{H}_{int}$:

- **One-photon interaction**: Only a one-photon interaction is considered, represented by the operator $\hat{\mathbf{A}}$ in equation (2.18). The term $\hat{\mathbf{A}}^2$ represents a two-photon interaction, whose effect would be much smaller than the one-photon interaction.

- **Dipole approximation**: The wavelength λ of the interacting electromagnetic field (≈ 1000 nm) is much larger than the size of the exciton extension ($a_s \approx 10$ nm)[3] and the size of the quantum dot, as is sketched in figure 2.4. Consequently, the position vector of the electron (hole) $\mathbf{r}_e$ is sufficiently defined by the position vector $\mathbf{r}_{qd}$ of the quantum dot $\mathbf{A}(\mathbf{r}_e) \approx \mathbf{A}(\mathbf{r}_{qd})$.

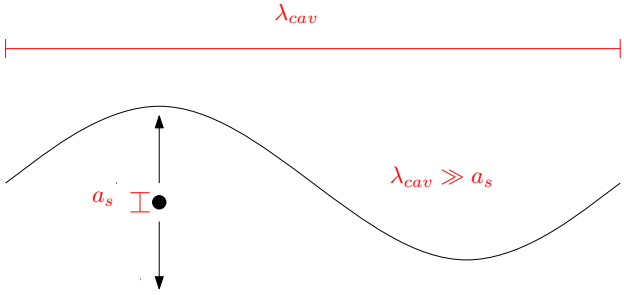

Figure 2.4: Scheme for dipole approximation

Furthermore, the momentum $\hat{\mathbf{p}}_e$ can be expressed as $\dot{\hat{\mathbf{r}}}_e = \hat{\mathbf{p}}_e/\mu$. Then the Heisenberg equation of motion reads

$$\hat{\mathbf{p}}_e = \frac{\mu}{i\hbar}[\hat{\mathbf{r}}_e, H_0] = \frac{\mu}{i\hbar}[\hat{\mathbf{r}}_e, H_{qd}]\,. \tag{2.20}$$

Projecting $\hat{\mathbf{p}}_e$ onto the two-state QD

$$\hat{\mathbf{p}}_e = \sum_{\alpha=g,e} \sum_{\alpha'=g,e} (|\alpha\rangle\langle\alpha|\hat{\mathbf{p}}_e|\alpha'\rangle\langle\alpha'|) \tag{2.21}$$

[3] $a_s = \hbar\kappa_s/(m_s e^2)$ is the *semiconductor Bohr* with strong dielectric screening κ_s in semiconductors and small electron and hole effective masses m_s [6].

and substituting with (2.19) we get

$$\hat{\mathbf{p}}_e = \frac{i\mu\omega_{qd}}{e}(\mathbf{d}_{ge}\hat{\sigma}_- - \mathbf{d}^*_{ge}\hat{\sigma}_+)\,, \tag{2.22}$$

with the atomic dipole matrix element

$$\mathbf{d}_{ge} \equiv -e\langle g|\mathbf{r}_e|e\rangle\,. \tag{2.23}$$

Now the interaction part of the Hamiltonian $\hat{H}_{int}$ reads

$$\hat{H}_{int} = i\hbar\sum_{\lambda=1}^{2}\sqrt{\frac{2\pi\omega_{qd}^2}{\hbar\omega_{cav}L^3}}(\mathbf{d}_{ge}\hat{\sigma}_- - \mathbf{d}^*_{ge}\hat{\sigma}_+)\cdot\left(\boldsymbol{\pi}_\lambda e^{i\mathbf{k}\cdot\mathbf{r}_{qd}}\hat{a}_\lambda + \boldsymbol{\pi}^*_\lambda e^{-i\mathbf{k}\cdot\mathbf{r}_{qd}}\hat{a}^\dagger_\lambda\right) \tag{2.24}$$

- **Rotating-wave approximation**($|\delta| \ll \omega_{cav}, \omega_{qd}$): If ω_{qd} and ω_{cav} are close to resonance we can neglect the rapidly oscillating terms in the interacting Hamiltonian [4], i.e., terms involving $e^{\pm 2i\omega_{qd}}$. As a consequence of this approximation the non resonant terms $\hat{\sigma}_+\hat{a}^\dagger_\lambda$ (creation of exciton and photon) and $\hat{\sigma}_-\hat{a}_\lambda$ (annihilation of exciton and photon), which are not energy preserving, can be neglected.

The Hamiltonian $H = \hat{H}_0 + H_{int}$ for a two-level-quantum dot in a cavity reads

$$H_0 = \hbar\omega_{qd}\hat{\sigma}_+\hat{\sigma}_- + \sum_{\lambda=1}^{2}\hbar\omega_{cav}\hat{a}^\dagger_\lambda\hat{a}_\lambda \tag{2.25}$$

and

$$H_{int} = i\hbar\sum_{\lambda=1}^{2}\left(g^*_\lambda\hat{a}^\dagger\hat{\sigma}_- - g_\lambda\hat{a}\hat{\sigma}_+\right) \tag{2.26}$$

$$g_\lambda = e^{-i\mathbf{k}\cdot\mathbf{r}_{qd}}\sqrt{\frac{2\pi\omega_{cav}}{\hbar L^3}}\boldsymbol{\pi}_\lambda\cdot\mathbf{d}^*_{ge} \tag{2.27}$$

with the dipole matrix element

$$\mathbf{d}_{ge} \equiv -e\langle g|\mathbf{r}_e|e\rangle\,. \tag{2.28}$$

The strength of the coupling between quantum dot and EM field depends on their relative spatial alignment $e^{-i\mathbf{k}\cdot\mathbf{r}_{qd}}$, the alignment of the polarization $\boldsymbol{\pi}_\lambda$ and the dipole direction $\mathbf{d}_{ge}$, and the mode volume of the cavity L^3.

For simplicity, we consider only linear polarization and a real polarization unit vector. This leads to more simple expressions

$$\boxed{\begin{aligned} H_0 &= \hbar\omega_{qd}\hat{\sigma}_+\hat{\sigma}_- + \hbar\omega_{cav}\hat{a}^\dagger\hat{a} && (2.29)\\ H_{int} &= g\hbar\left(\hat{a}^\dagger\hat{\sigma}_- + \hat{a}\hat{\sigma}_+\right) && (2.30)\end{aligned}}$$

These Hamiltonians are employed in the further discussion.

[4] This approximation is convincing when transforming the system into the Dirac interaction picture

2.4.2 Polaritonic states

Now, we are going to solve the coupled QD-cavity-system. Its Hamiltonian consists of equation(2.29) and equation(2.30). The solution of H_0 is already derived in section 2.3.

The pair $\{|g\rangle \otimes |n\rangle, |e\rangle \otimes |n\rangle : n \in \mathbb{N}_0\}$ builds an orthogonal basis of the $\mathcal{H} = \mathcal{H}_{qd} \otimes \mathcal{H}_{cav}$ Hilbert space. The matrix elements of H are given by $\langle a| \otimes \langle n|\hat{H}|a'\rangle \otimes |n'\rangle$ with $a = \{g, e\}$. g denotes the ground state and e denotes the excited state of the exciton. The resulting matrix is *block-diagonal*. The elements of the diagonal are the ground state $E_{g,0} = 0$ and the square matrices H_n.

$$H_{i,j} = \begin{pmatrix} E_{g,0} & 0 & \cdots & & 0 \\ 0 & H_1 & & & \\ & & H_2 & & \vdots \\ \vdots & & & \ddots & \\ & & & H_n & 0 \\ 0 & & \cdots & 0 & \ddots \end{pmatrix}. \tag{2.31}$$

This matrix is an infinite-dimensional matrix if the number of photons n is not limited. To diagonalize the matrix H it is sufficient to diagonalize the 2-dimensional subspaces H_n:

$$H_n = \begin{pmatrix} \langle e| \otimes \langle n-1|\hat{H}|e\rangle \otimes |n-1\rangle & \langle e| \otimes \langle n-1|\hat{H}|g\rangle \otimes |n\rangle \\ \langle g| \otimes \langle n|\hat{H}|e\rangle \otimes |n-1\rangle & \langle g| \otimes \langle n|\hat{H}|g\rangle \otimes |n\rangle \end{pmatrix} \tag{2.32}$$

$$= \begin{pmatrix} E_{e,n-1} & \omega_n\hbar/2 \\ \omega_n\hbar/2 & E_{g,n} \end{pmatrix}, \; n \geq 1$$

with

$$\omega_n = 2g\sqrt{n} \tag{2.33}$$

being the n^{th} *resonant Rabi-frequency.*

Energy-eigenvalues of H_n

$$E_{1,n} = \frac{(E_{g,n} + E_{e,n-1})}{2} + \frac{\hbar}{2}\sqrt{\delta^2 + \omega_n} = \frac{(E_{g,n} + E_{e,n-1})}{2} + \frac{\hbar}{2}\Omega_n, \tag{2.34}$$

$$E_{2,n} = \frac{(E_{g,n} + E_{e,n-1})}{2} - \frac{\hbar}{2}\sqrt{\delta^2 + \omega_n} = \frac{(E_{g,n} + E_{e,n-1})}{2} - \frac{\hbar}{2}\Omega_n \tag{2.35}$$

with

$$\Omega_n \equiv \sqrt{\delta^2 + \omega_n} \tag{2.36}$$

is known as the *general Rabi-frequency,*and is shown for $n = 1$ in figure 2.5.

The interval $\hbar\Omega_n$ of the two eigenstates of H_n is termed *Rabi mode splitting.* In time resolved calculations we get *vacuum Rabi oscillations*, see fig 2.6.

Eigenstates of H_n

$$|1, n\rangle = \sin(\vartheta_n)|e\rangle \otimes |n-1\rangle + \cos(\vartheta_n)|g\rangle \otimes |n\rangle \tag{2.37}$$

$$|2, n\rangle = \cos(\vartheta_n)|e\rangle \otimes |n-1\rangle - \sin(\vartheta_n)|g\rangle \otimes |n\rangle \tag{2.38}$$

with

$$\tan(2\vartheta_n) = \frac{\omega_n}{\delta}. \tag{2.39}$$

As can be seen in equations (2.37) and (2.38) the state of the exciton is entangled with the state of the cavity mode, forming *polaritonic* eigenstates. These states are also termed *dressed states*, because the states of exciton and cavity-mode build a composite state that cannot be separated anymore in exciton or cavity-mode. The "dressed" exciton is a quasi-particle and can be termed **exciton-polariton**. The entanglement of exciton-field states is maximal when $\omega_{qd} = \omega_{cav}$. Then the eigenstates read $\frac{1}{\sqrt{2}}(|e\rangle \otimes |n-1\rangle \pm |g\rangle \otimes |n\rangle)$.

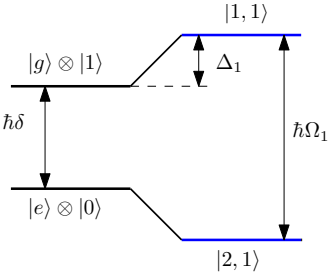

Figure 2.5: Energy splitting of the uncoupled and the coupled QD-cavity system.

In figure 2.5 we see the energy-splitting of the uncoupled states $|g\rangle \otimes |n\rangle$ and $|e\rangle \otimes |n-1\rangle$ and the dressed states $|1,n\rangle$ and $|2,n\rangle$, for $n = 1$. The energy splitting of the uncoupled system is already discussed in section 2.3 and shown in figure 2.3. Compared to the uncoupled QD-cavity system the energy splitting increases $2\Delta_1 = \hbar(\Omega_1 - \delta)$ for the coupled case. The two dressed states are separated by an interval of $\hbar\Omega_1$, i.e., the first Rabi mode splitting.

Rabi Oscillation

The Hamiltonian in the dressed state basis is not explicitly time dependent. So the general time evolution reads

$$|\Psi(t)\rangle = \sum_n \left(c_{1,n}|1,n\rangle e^{-iE_{1,n}t/\hbar} + c_{1,n}|2,n\rangle e^{-iE_{2,n}t/\hbar}\right) \tag{2.40}$$

When the exciton is in the excited state $|\Psi(0)\rangle = |e\rangle \otimes |0\rangle$ for the initial condition $(t = 0)$ then the time dependent probability $P_e(t)$ for exciton excitation reads

$$P_e(t) = \frac{\omega_n}{\Omega_n} \cos^2\left(\frac{g}{\hbar}\sqrt{n}t\right) =_{\delta=0} \cos^2\left(\frac{g}{\hbar}\sqrt{n}t\right) \tag{2.41}$$

As can be seen in figure 2.6 the exciton state is excited with an oscillating

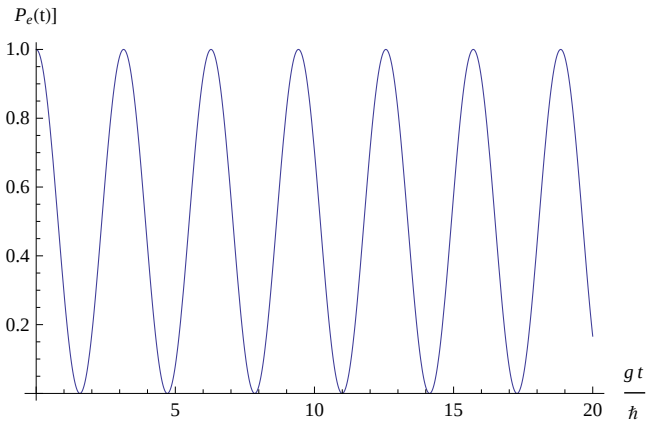

Figure 2.6: Probability $P_e(t)$ that the exciton is excited for $\delta = 0$ (Rabi oscillation for n=1).

probability. The excitation energy oscillates between the quantum dot and the cavity with the Rabi frequency ω_n. Thus the time dependent probability of the cavity mode $P_{cav}(t)$ is for the ideal case

$$P_{cav}(t) = 1 - P_e(t). \tag{2.42}$$

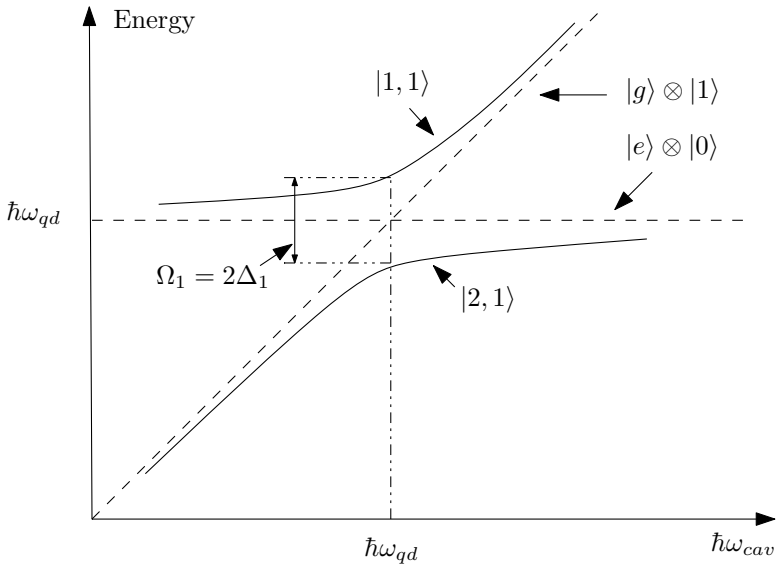

Figure 2.7: Energy of the polaritonic states $|1,1\rangle$ and $|2,1\rangle$ (solid lines) versus $\hbar\omega_{cav}$. The dashed lines represent the uncoupled states $|e\rangle \otimes |n-1\rangle$ and $|g\rangle \otimes |n\rangle$.

2.4.3 Anticrossing for $\omega_{cav} \approx \omega_{qd}$

Anticrossing for n=1

Consider a quantum dot with constant energy $\hbar\omega_{qd}$ and a cavity with a tunable resonance energy $\hbar\omega_{cav}$. Figure 2.7 shows the principal behavior of system energy versus cavity energy for the uncoupled and the coupled case. The dashed lines in the graph show the energy of the uncoupled system of one manifold, here $|e\rangle \otimes |n-1\rangle$ and $|g\rangle \otimes |n\rangle$. They intersect at $\hbar\omega_{cav} = \hbar\omega_{qd}$.

As is well known from the classical model of two coupled oscillators, mode splitting occurs when the resonance energies of both oscillators are similar. Also here, anticrossing can be observed for the coupled system shown by the solid lines in the graph. In contrast to the uncoupled system there is no intersection of $|1,1\rangle$ and $|2,1\rangle$. The uncoupled-energy-lines act as asymptotes for energies far from $\omega_{cav} = \omega_{qd}$. The minimum distance $\hbar\Omega_1 = 2\Delta_1$ is found for $\hbar\omega_{cav} = \hbar\omega_{qd}$. Detuning of the cavity results in an increasing distance of the tow states.

When the detuning $\delta = \omega_{cav} - \omega_{qd}$ changes from positive values to negative values, the state $|1,1\rangle$ passes continuously from the uncoupled state $|e\rangle \otimes |0\rangle$ with $\hbar\omega_{qd}$ (constant QD energy) to the uncoupled state $|g\rangle \otimes |1\rangle$ with $\hbar\omega_{cav}$ (tunable cavity energy). For $\delta = 0$, a linear superposition of these two states can be seen with equal weights $|1,1\rangle = \frac{1}{\sqrt{2}}(|e\rangle \otimes |0\rangle + |g\rangle \otimes |1\rangle)$.

Anticrossing for n=1,2

Now we calculate with equation (2.34) and 2.35 the eigen-energies of the lowest polaritonic states $|1, n\rangle$ and $|2, n\rangle$ for $n = 1, 2$. The Jaynes-Cummings model predicts a characteristic nonlinear scaling of the vacuum Rabi oscillation frequency as $\omega_n = 2\sqrt{n}g$ with the number of excitation n in the system at resonance. This quantum effect is in stark contrast to the normal mode splitting of two classical coupled linear oscillators, which is independent of the oscillator amplitude [3].

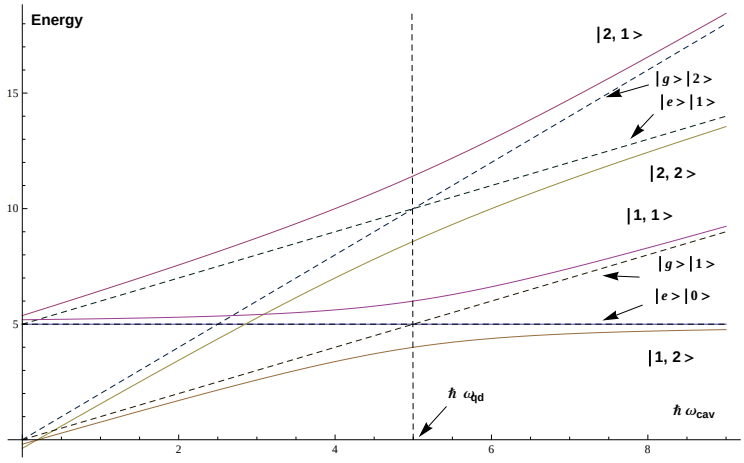

Figure 2.8: Anticrossing of the coupled QD-cavity system calculated with the Jaynes-Cummings model.

Figure(2.8) shows anti-crossings of the first and second duplet, $\{|1, 1\rangle, |2, 1\rangle\}$ and $\{|1, 2\rangle, |2, 2\rangle\}$. Cavity-energy is plotted versus the total energy. The uncoupled first and second duplet intersect at the same cavity energy $\hbar\omega_{cav}$. For the 2^{nd} duplet we find the nonlinear value of the energies $2\sqrt{2}g\hbar$. Up to now experimental evidence of this phenomenon is only reported for the atom-cavity system [3]. For the QD-cavity system discussed here measurements are still missing.

Until now an idealized system is discussed where losses are not considered. In real coupled systems it is necessary to take further effects into account that are generally not coherent.

Further effects

- **Dissipative effects** We have to consider our system being in contact with its environment E which can lead to *loss-mechanisms* but also to gain (pumping). A way to formulate this fact is done by the *master equation of Lindblad form*, a special formalism for open quantum system which will be explained in the next chapter.

- **QD-phonon-coupling** Measurements showed a strong cavity peak despite large detuning of exciton and cavity that cannot be explained only

by cavity-exciton interaction. A possible decay channel is the coupling of the system to phonons in the environment as has been shown recently by Hohenester [8, 7]. This effect is discussed in chapter 4 and 5.

Chapter 3

Open Quantum System

In this chapter we are characterizing a "real" QD-cavity system, that includes optical losses of the cavity mode (κ) and spontaneous decay of the exciton (γ) into optical modes outside the cavity. Thus the ideal QD-cavity system interacts with an external quantum system - the infinitely large environment reservoir R.

3.1 Density Matrix $\hat{\rho}$

The following description of the density matrix is based on [1] and [10].

Consider an open quantum system with several possible states. Due to the dissipative nature of an open system one does not know the exact state of the quantum system, but only the classical[1] probabilities of the possible system states. Thus such an open quantum system can only be described by a density matrix $\hat{\rho}$, while a closed quantum system can be equivalently modeled with the state $|\psi\rangle$ or the density matrix $\hat{\rho}$.

We start describing a closed system S in state $|\psi\rangle$. The complete basis of the closed system is $|e_i\rangle$, where $\sum_i |e_i\rangle\langle e_i| = \mathbb{1}$ with $\mathbb{1}$ being the unit operator. The expectation values $\langle\hat{A}\rangle$, that describe measurable quantities, read

$$\begin{aligned}\langle\hat{A}\rangle &= \langle\psi|\hat{A}|\psi\rangle \\ &= \sum_i \langle\psi|\hat{A}|e_i\rangle\langle e_i||\psi\rangle \\ &= \sum_i \langle e_i|\psi\rangle\langle\psi|\hat{A}|e_i\rangle \\ &= Tr(\hat{\rho}\hat{A})\end{aligned} \tag{3.1}$$

where $\hat{\rho} = |\psi\rangle\langle\psi|$ is the density matrix.[2] So, as an alternative to $|\psi\rangle$, the system can also be described with $\hat{\rho}$. Both descriptions are equivalent for a closed

[1] The system is in a definite quantum state, although we do not know which state.[2]

[2] For detailed properties of $\hat{\rho}$ see [9].

quantum system. In contrast, an open quantum system does not posses definite states $|\psi\rangle$, however its density matrix $\hat{\rho}$ can be defined. The equivalent to the Schrödinger equation is the *von-Neumann equation* for the time evolution of $\hat{\rho}$

$$\frac{\partial}{\partial t}\hat{\rho} = -\frac{i}{\hbar}[\hat{H}, \hat{\rho}]. \tag{3.2}$$

3.1.1 Composite closed quantum system

An open quantum system can be described by defining a "large" composite closed system, that consists of a small open quantum system and its large environment. The Hamiltonian of the composite system $H_{S\otimes R} = H_S + H_R + H_{RS}$ consists of the Hamiltonian H_S of the open system S, the Hamiltonian H_R of the reservoir R and their interaction Hamiltonian H_{RS}. As noted above for equation (3.2), the time evolution of the density operator $\hat{\rho}(t)$ is described by the master equation. In the Schrödinger picture the corresponding master equation is known as the *von-Neumann equation*

$$\frac{\partial}{\partial t}\hat{\rho} = -\frac{i}{\hbar}[\hat{H}_{S\otimes R}, \hat{\rho}]. \tag{3.3}$$

For our purpose, namely getting a master equation that describes the QD-cavity system with its loss mechanism, it is convenient to use the interaction picture. In the interaction picture the master equation reads

$$\dot{\tilde{\hat{\rho}}}(t) = \frac{1}{i\hbar}\left[\tilde{\hat{H}}_{SR}(t), \tilde{\hat{\rho}}(t)\right] \tag{3.4}$$

with the corresponding density matrix $\tilde{\hat{\rho}}(t)$

$$\tilde{\hat{\rho}}(t) \equiv e^{\frac{i}{\hbar}(H_S+H_R)t}\hat{\rho}(t)e^{-\frac{i}{\hbar}(H_S+H_R)t} \tag{3.5}$$

and the interaction Hamiltonian $\tilde{H}_{SR}(t)$ for the interaction picture

$$\tilde{H}_{SR}(t) \equiv e^{\frac{i}{\hbar}(H_S+H_R)t}H_{SR}e^{-\frac{i}{\hbar}(H_S+H_R)t}. \tag{3.6}$$

Integrating (3.4) and doing some substitution the time evolution of the density matrix $\tilde{\hat{\rho}}(t)$ reads

$$\dot{\tilde{\hat{\rho}}}(t) = \frac{1}{i\hbar}\left[\tilde{H}_{SR}(t), \tilde{\hat{\rho}}(0)\right] - \frac{1}{\hbar^2}\int_0^t ds\left[\tilde{H}_{SR}(t), \left[\tilde{H}_{SR}(t-s), \tilde{\hat{\rho}}(t-s)\right]\right], \tag{3.7}$$

written in integro-differential form. This equation constitutes the general description of the composite quantum system. The complexity of the reservoir makes it impossible to solve this equation. However, the problem can be solved for the reduced density operator $\tilde{\hat{\rho}}_S$ of the open system S, the dynamic of which we are interested in.

Reduced density operator $\hat{\rho}_S$

The reduced density operator $\hat{\rho}_S$ describes the system S without including any detailed information on the reservoir. It is defined by taking a partial trace over the reservoir variables of the density operator of the composite system

$$\hat{\rho}_S(t) \equiv tr_R\{\hat{\rho}(t)\}. \tag{3.8}$$

The time evolution of the reduced density operator $\hat{\rho}_S(t)$ is governed by the master equation

$$\dot{\tilde{\hat{\rho}}}_S(t) = \frac{1}{i\hbar} tr_R\Big\{\Big[\tilde{H}_{SR}(t), \tilde{\hat{\rho}}(0)\Big]\Big\} - \frac{1}{\hbar^2}\int_0^t ds\; tr_R\Big\{\Big[\tilde{H}_{SR}(t), \Big[\tilde{H}_{SR}(t-s), \tilde{\hat{\rho}}(t-s)\Big]\Big]\Big\}. \tag{3.9}$$

As this equation still includes the density operator of the composed system $\tilde{\hat{\rho}}(t)$, it is still not solvable. Further approximations have to be introduced to obtain a solvable equation for $\tilde{\hat{\rho}}_S(t)$:

1. The open system and the reservoir are initially uncorrelated and the reservoir is in equilibrium; $\tilde{\hat{\rho}}(0) = \varrho_0 \tilde{\hat{\rho}}_S(0)$, where ϱ_0 is the density operator of the reservoir at $t = 0$.

2. Interaction has no diagonal elements; $tr_R\Big\{\Big[\tilde{H}_{SR}(t), \varrho_0\Big]\Big\} = 0$.

3. The coupling between S and R is weak enough that the contributions of interaction processes higher than second-order can be neglected (*Born approximation*). $\tilde{\hat{\rho}}(t)$ deviates from uncorrelated system only in first or second order of H_{SR},

$$\tilde{\hat{\rho}}(t) = \varrho_0 \tilde{\hat{\rho}}_S(t) + \mathcal{O}(H_{SR}). \tag{3.10}$$

$$\dot{\tilde{\hat{\rho}}}_S(t) = -\frac{1}{\hbar^2}\int_0^t ds\; tr_R\Big\{\Big[\tilde{H}_{SR}(t), \Big[\tilde{H}_{SR}(t-s), \varrho_0 \tilde{\hat{\rho}}_S(t-s)\Big]\Big]\Big\}. \tag{3.11}$$

   This is the master equation in *Born approximation* because of $\tilde{\hat{\rho}}_S(t-s)$ it still contains retardation effects.

4. Internal correlations in R are on a much shorter time scale than the relaxation of S (*Markov approximation*). So $\tilde{\hat{\rho}}_S(t-s)$ can be replaced by $\tilde{\hat{\rho}}_S(t)$; excludes memory effects.

5. The upper integration limit t becomes infinite. (*Adiabatic approximation*)

6. For the next step we have to expand the interaction Hamiltonian in terms of eigenoperators of the systems Hamiltonian and substitute the new interaction Hamiltonian into the approximated master equation.

7. Terms in the interaction Hamiltonian that oscillate much more rapidly than the others are neglected (*Secular approximation*).

These approximations and the introduction of an effective Hamiltonian [10] lead to the master equation in *Lindblad form*.

3.2 Master Equation in Lindblad form

The Lindblad equation or master equation in the Lindblad form is the most general type of markovian and time-homogeneous master equation. It describes a non-unitary time evolution[3] of the density matrix $\hat{\rho}$ that is trace preserving and completely positive for any initial condition.

$$\dot{\hat{\rho}}_S = -\frac{i}{\hbar}[H, \hat{\rho}_S] + \sum_k \gamma_k \left[A_k \hat{\rho}_S A_k^\dagger - \frac{1}{2}\{\hat{\rho}_S, A_k^\dagger A_k\} \right] \tag{3.12}$$

- The first part of the equation ($-\frac{i}{\hbar}[H, \hat{\rho}_S]$) describes the coherent part of the dynamics. $\hat{H}$ is the system Hamiltonian.
- The second part describes incoherent processes as dissipation. A_k is the Lindblad operator. γ_k is a non-negative quantity that accounts for relaxation rates of different decay channels of the system and is defined by a correlation function of the reservoir.

The equation is *Markovian*, thus we neglect memory effects of the reservoir.

3.2.1 QD-cavity system with losses

Besides the coherent cavity-QD-coupling loss-mechanisms have to be considered for excitons and cavity photons. The main loss mechanisms are described by relaxation rate of the QD due to spontaneous emission into EM field modes other than the cavity mode γ and the photon loss rate of the cavity mode

$$\kappa = \omega_{cav}/Q \tag{3.13}$$

which depends on the resonance frequency ω_{cav} and the quality factor Q of the cavity.

[3] closed systems do evolve unitary in time

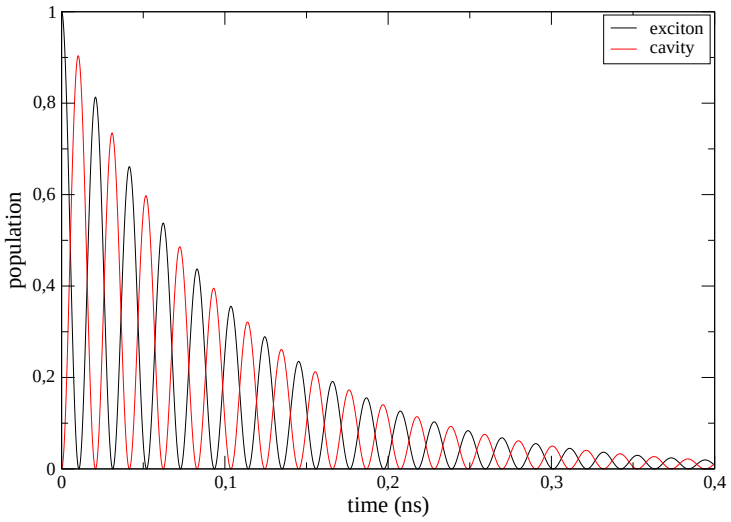

Figure 3.1: QD-cavity system with losses. Coupling constant $g = 100\,\mu eV$, QD decay $\gamma = 0.16\,\mu eV$ and cavity decay $\kappa = 13\,\mu eV$.

Generally, the coupling between the QD and the cavity mode can be strong or weak, depending on on the balance between the coherent coupling rate g and the dissipation rates γ and κ. We are interested in strongly coupled systems where coherent cavity-QD-coupling g dominates and

$$\frac{\kappa + \gamma}{2} < 2g \tag{3.14}$$

is satisfied. Such an open exciton-cavity system shows the oscillating coupling properties of an ideal closed system discussed in section 2.2, however with an additional damping which decreases the oscillation between exciton and cavity mode exponentialy in time, as can be seen in figure 3.1.

$$A_e = \sqrt{\gamma}\ |g\rangle\langle e| \otimes \mathbb{1} \tag{3.15}$$

$$A_{cav} = \sqrt{\kappa}\ \mathbb{1} \otimes |0\rangle\langle 1| \tag{3.16}$$

A_e and A_{cav} are the Lindblad operators of the exciton and cavity.

Chapter 4

Phonon assisted Cavity Feeding

Generally, QD-cavity coupling demands low detuning of the exciton and the cavity mode. However, PL measurements showed a strong cavity emission even when tuning the system far off-resonant. This PL peak only appears for QD-cavity systems, while it is not evident for empty cavities [11]. This phenomenon can be explained by phonon scattering in the host matrix. More precisely, cavity feeding is caused by a combined effect of exciton-cavity and exciton-phonon coupling, where the exciton decays into a cavity photon and the energy mismatch is compensated by the emission or absorption of a phonon.

In the theoretical model this effect can be included as an additional decay channel. This is done by adding a third incoherent term $A_{phon-ass}$ to the Lindblad equation (3.12)

$$\hat{A}_{phon-ass} = \sqrt{\Gamma}|1;g\rangle\langle 0;e|, \tag{4.1}$$

that accounts for the decay $|0;e\rangle$ to $|1;g\rangle$, with a scattering rate Γ. In contrast to the exciton and the cavity decay discussed in chapter 3, this scattering rate is not constant, but depends on temperature and detuning.

4.1 Phonon assisted scattering rate Γ

Γ can be modeled with the general Fermi Golden Rule approach, that allows to calculate the transition rate from an initial state into the continuum of states of the system by means of a time-dependent perturbation.

4.1.1 Hamiltonian

Again we divide our system into the free part H_0 and the interaction part H_{int}

$$H = H_0 + H_{int} \tag{4.2}$$

Phonon interaction is taken into account by introducing free phonon bath $\hat{H}_{ph}$ and exciton-phonon coupling $\hat{H}_{ep}$. The free phonon bath

$$\hat{H}_{ph} = \sum_k \hbar\omega_k b_k^\dagger b_k, \tag{4.3}$$

is described by b_k being the bosonic annihilation operator and $\hbar\omega_k$ being the energy of the k^{th} phonon mode. Exciton-phonon coupling is described by

$$\hat{H}_{ep} = |g\rangle\langle g|B_{gg} + |e\rangle\langle e|B_{ee}, \tag{4.4}$$

with

$$B_{gg} = \sum_k \lambda_{gg,k}\left(b_k + b_k^\dagger\right) \tag{4.5}$$

$$B_{ee} = \sum_k \lambda_{ee,k}\left(b_k + b_k^\dagger\right) \tag{4.6}$$

known as the bath operators B_{gg} and B_{ee} where $\lambda_{gg,k}$ and $\lambda_{ee,k}$ are the electron phonon matrix elements, containing the strength of coupling. Then the Hamiltonian consists of

$$\hat{H}_0 = \hat{H}_{qd} + \hat{H}_{cav} + \hat{H}_{ph} \tag{4.7}$$

$$= \hbar\omega_{qd}\hat{\sigma}_+\hat{\sigma}_- + \hbar\omega_{cav}\hat{a}^\dagger\hat{a} + \sum_k \hbar\omega_k b_k^\dagger b_k \tag{4.8}$$

and

$$H_{int} = \hat{H}_g + \hat{H}_{ep} \tag{4.9}$$

$$= g\hbar\left(\hat{a}^\dagger\hat{\sigma}_- + \hat{a}\hat{\sigma}_+\right) + |g\rangle\langle g|B_{gg} + |e\rangle\langle e|B_{ee}. \tag{4.10}$$

4.1.2 General Fermi's Golden Rule

The Fermi's golden rule describes transition rates of an initial state $|i\rangle$ of a quantum system into a continuous spectrum of final states due to first-order time-dependent perturbation theory [4]. Here the Hamiltonian

$$\hat{H} = \hat{\bar{H}}_0 + V \tag{4.11}$$

consists of an exactly solvable part $\bar{H}_0$ and a small perturbation V. While several approaches exist where different parts of the interaction are treated as the perturbation [4], we choose the exciton-phonon interaction hamiltonian $\hat{H}_{ep}$.

The computation of the phonon-assisted scattering rates is approximated by the master equation in Born approximation, where retardation is included, as

derived in chapter 3. Now the QD-cavity system $\hat{\rho}_s$ is embedded in a reservoir of phonons $\hat{\rho}_{ph}$

$$\dot{\hat{\rho}}_s \approx -\int_{t_0}^{t} tr_{ph}\Big([V(t),[V(\tau),\hat{\rho}_s(t)\otimes\hat{\rho}_{ph}]]\Big)d\tau, \tag{4.12}$$

where $V(t)$ is the perturbation in the interaction representation of $\bar{H}_0$. We consider the transition between initial state (excited exciton) $|e;0\rangle$ and the final state (cavity photon) $|g;1\rangle$. In particular we aim to calculate the time dependent evolution of the density of the final state $\hat{\rho}_{S_{ff}}$, which is an element of the diagonal of the density matrix $\hat{\rho}_s$. As already discussed in section 3.1.1 the following assumptions have to be introduced to obtain a solvable master equation in Born approximation:

1. The open system S and the phonon reservoir R are initially uncorrelated and the reservoir is in equilibrium.

2. The coupling between S and R is weak enough that the contributions of interaction processes higher than second-order can be neglected (*Born approximation*).

With adiabatic approximation and further approximations [7], the expression can be brought into the form

$$\hat{\rho}_{S_{ff}} = \Gamma_{if}\hat{\rho}_{S_{ii}} \tag{4.13}$$

where $\hat{\rho}_{S_{ii}}$ is a diagonal matrix element of $\hat{\rho}_S$. Finally, we obtain the scattering rate Γ_{if} for the phonon assisted decay $|e,0\rangle \longrightarrow |g,1\rangle$ expressed in the generalized Fermi golden rule

$$\Gamma_{if} = 2Re\int_{-\infty}^{0} tr_{ph}\left(\hat{\rho}_{ph}\langle i|V(\tau)|f\rangle\langle f|V(0)|i\rangle\right). \tag{4.14}$$

To be able to calculate the scattering rate, still, the perturbation term V has to be derived. This can be done with the *Schrieffer-Wolff transformation*.

4.1.3 Schrieffer-Wolff transformation

For off-resonant decay, exciton-cavity and exciton-phonon coupling are relevant for the scattering rate. According to equation (4.11), $H = \bar{H}_0 + V$, we write

$$\bar{H}_0 = H_0 + H_g \tag{4.15}$$

$$V = H_{ep} \tag{4.16}$$

where we treat $\bar{H}_0 = H_0 + H_g$ as the exactly solvable part of the Hamiltonian and H_{ep} as perturbation. Applying the Schrieffer-Wolff transformation

$$\tilde{H} = e^s H e^{-s} = H + [s, H] + \frac{1}{2}[s, [s, H]] + ..., \tag{4.17}$$

$$\approx \tilde{\bar{H}}_0 + \tilde{H}_{ep} \tag{4.18}$$

allows us to reduce the exciton-cavity coupling to the lowest order of g, when s solves $[s, H_0] + H_g = 0$ with the operator $s = \frac{g}{\Delta}\left(\sigma_+ a - \sigma_- a^\dagger\right)$. Δ is the detuning between exciton and cavity. This unitary transformation leads to $\bar{H}_0 = H_0 + O(g^2)$. The second order term $O(g^2)$ corresponds to Lamb and Stark shifts and can be neglected

$$\tilde{\bar{H}}_0 \approx H_0 \tag{4.19}$$

Thus, the transformation provides a simple expression for $\tilde{\bar{H}}_0$, while H_g only is included in the transformed perturbation part $\tilde{H}_{ep}$

$$\tilde{H}_{ep} \approx H_{ep} - \frac{g}{\Delta}\left(\sigma_+ a - \sigma_- a^\dagger\right)\left(B_{ee} - B_{gg}\right), \tag{4.20}$$

where the second term $\frac{g}{\Delta}\left(\sigma_+ a - \sigma_- a^\dagger\right)\left(B_{ee} - B_{gg}\right)$ describes the combined interaction of H_g and H_{ep}. This perturbation $\tilde{H}_{ep}$ can be inserted into equation (4.14) as our perturbation V. Considering our system being in thermal equilibrium, only phonon occupations $\langle b_k^\dagger b_k \rangle = \bar{n}_k$ are non-zero, where the occupation is given by the Bose-Einstein-statistic

$$\bar{n}_k = \frac{1}{\exp[\frac{\hbar\omega_k}{k_B T}] - 1}. \tag{4.21}$$

Finally, we obtain the scattering rate for a QD-Cavity-system with phonon interaction

$$\Gamma_{eg} = (\frac{g}{\Delta})^2 2\pi \sum_k |\lambda_{ee,k} - \lambda_{gg,k}|^2 \big(\bar{n}_k \quad \delta(\Delta + \omega_k) + (\bar{n}_k + 1)\delta(\Delta - \omega_k)\big). \tag{4.22}$$

The scattering rate Γ_{eg} depends on the strength of exciton-cavity coupling g and exciton-phonon coupling $|\lambda_{ee,k} - \lambda_{gg,k}|$, on the detuning Δ and the temperature T.

Chapter 5

Calculations

In this section calculations are presented that model a QD-cavity-system embedded in a phonon reservoir for varying temperature and detuning. We start with the simple case of a resonant system without considering losses, detuning and phonon scattering. Then we introduce these elements step by step and discuss their influence on the population of the exciton and the cavity.

The calculations are performed using the codes of U. Hohenester [7, 8]. For some plots the codes have been slightly modified. These codes were derived with an approach (*Independent Boson Model*) that deviates from the approach discussed before. While in this work, the focus was laid on a straight forward solution of the problem, the discussion of the Independent Boson Model would require a more detailed description. The solutions for both approaches are similar [7].

For all calculations we assume for the initial state (time $t = 0$) an excited exciton $|0; e\rangle$ and no cavity-photon $|1; g\rangle$. The values used for the calculations can be found in table 5.1 on page 37, unless stated differently.

5.1 Detuning

5.1.1 No losses, detuning, no phonon scattering

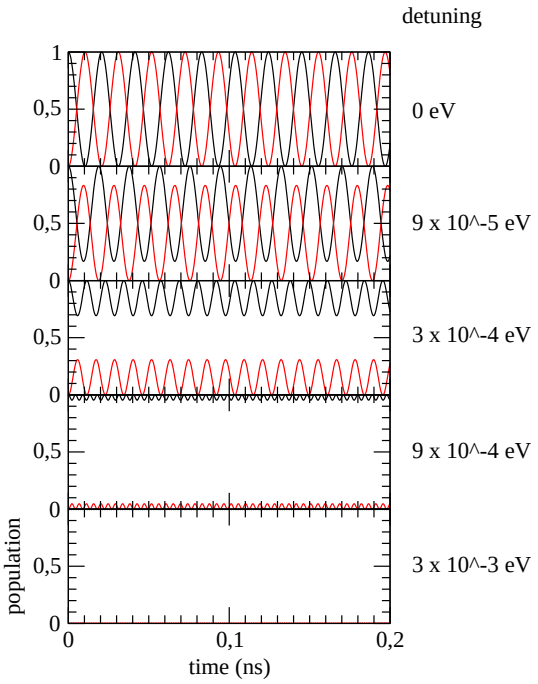

Figure 5.1: Population of the exciton (black lines) and the cavity (red lines) for the resonant case ($\hbar\omega_{qd} = \hbar\omega_{cav} = 1.3\,eV$) and for increasing detuning Δ. No losses and no phonon scattering are considered.

We model the QD-cavity system with the Jaynes-Cummings Modell; no loss mechanisms and no phonon effects. These assumptions constitute the ideal case of a purely coherent system. The time dependend population of the exciton and the cavity for the resonant case $\omega_{qd} = \omega_{cav}$ and for increasing detuning

$$\Delta = \hbar(\omega_{qd} - \omega_{cav}) \tag{5.1}$$

can be seen in figure 5.1. The populations follow the equations

$$P_{qd}(t) = 1 - \frac{\omega^2}{\Omega^2}\sin^2(\frac{1}{2}\Omega t), \tag{5.2}$$

$$P_{cav}(t) = \big(1 - P_{qd}(t)\big) = \frac{\omega^2}{\Omega^2}\sin^2(\frac{1}{2}\Omega t), \tag{5.3}$$

where ω is the resonant Rabi frequency and

$$\Omega = \sqrt{\Delta^2 + \omega^2} \tag{5.4}$$

is the general Rabi frequency.

The resonant system ($\Delta = 0\,eV$) is strongly oscillating between the cavity and the excitonic state, where maximum population of the exciton coincides with a zero minimum for the cavity population, and vice versa. As already shown in figure 2.6 we observe periodically an excitonic or a cavity state with propability $P = 1$. When the QD is detuned with respect to the cavity the minima of the population of the exciton are no longer zero and the maximum population of the cavity is below 1, while we still observe periodically excitonic state with propability $P = 1$. Thus the population transfer from the exciton to the cavity is reduced. Large detuning ($\Delta = 3meV$) results in a very low propability for a cavity photon, in other words the exciton remains excited.

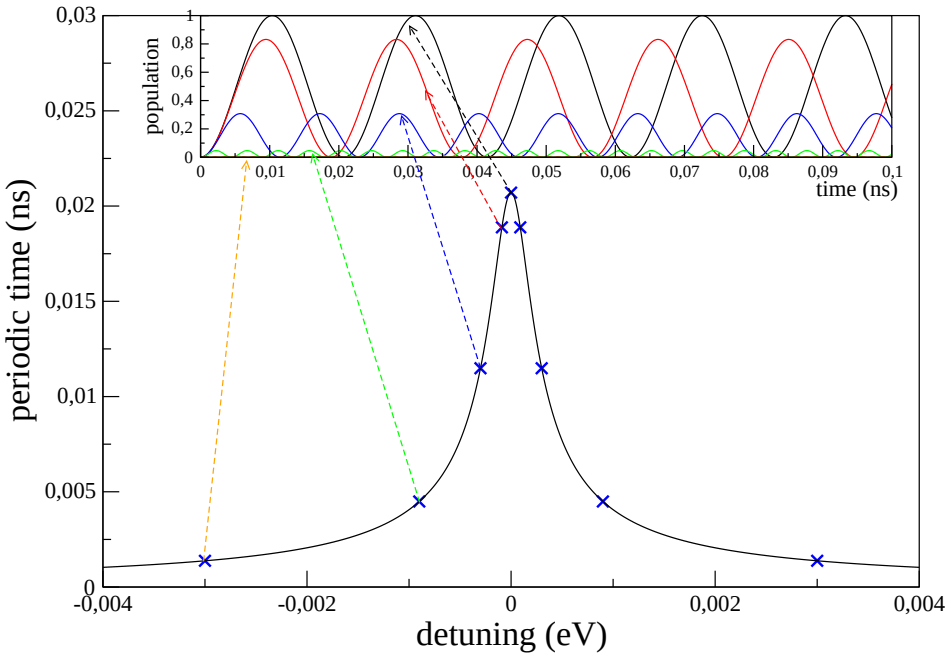

Figure 5.2: Periodic time for the QD-cavity oscillation versus detuning Δ. The curves in the inset steem from figure 5.1 and show the population of the cavity for $\Delta = 0\,eV$ and increasing detuning.

Turning now to the frequency Ω of the oscillating populations, we observe higher frequency for increasing detuning, see equation 5.4. Thus, the time period

is maximum for the resonant case, as is shown in figure 5.2. This effect can also be seen in figures 5.7 and 5.8, discussed later in this chapter. Note, that the other parameters discussed in the following (losses and phonon scattering) do not influence the time period significantly.

The amplitudes of the oscillating populations decrease when tuning the system more off resonance, as is evident from equations 5.2, 5.3 and 5.4.

Concluding, we observe that detuning leads to a vanishing cavity population. Experiments, however, showed a significant cavity signal for off resonant QD cavity systems [5, 11]. The origin of these experimentally detected cavity photons despite large detuning, will be discussed in the following sections.

5.2 Losses

5.2.1 Losses, no detuning, no phonon scattering

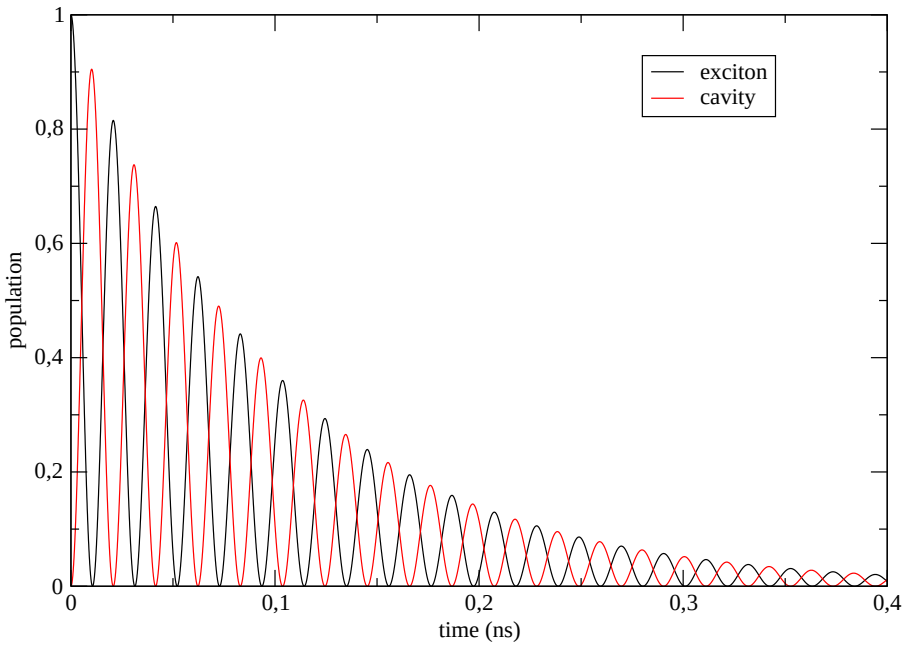

Figure 5.3: Population of the exciton (black line) and the cavity (red line) for the resonant case with cavity losses $\kappa = \omega_{cav}/Q$, no detuning and no phonon scattering are considered.

In figure 5.3 we can see the time dependend populations of the exciton and the cavity photon for a resonant QD-cavity system including cavity losses κ. QD losses play a minor role and are not considered in this work. The populations show the same behavior as for the resonant case in figure 5.1, but due to the losses the amplitudes decrease exponentially in time. Thus, we still have periodical pure excitonic and pure cavity states, but with a decreasing propability $P(t)$.

More complex behavior is observed when detuning and/or phonon scattering become significant as discussed in the following.

5.2.2 Losses, detuning, no phonon scattering

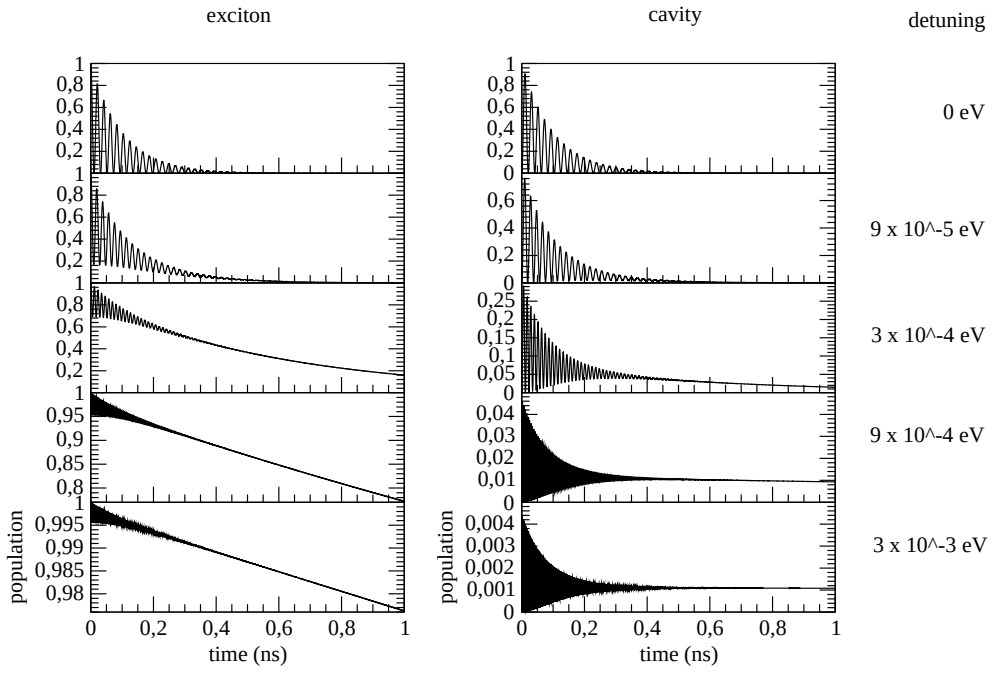

Figure 5.4: Population of the exciton and the cavity for increasing detuning, with losses but without phonon scattering. Mind the different scales of the populations for increasing detuning.

The influence of detuning on the populations when losses are considered can be seen in figure 5.4. Still no phonon scattering is assumed. In contrast to figure 5.1, detuning affects both, the minima and the maxima, of the populations. The lifetime of the exciton is considerably shorter (faster decay of the maxima) in resonance. This can be understood, because in resonance cavity losses are more effective due to a larger population transfer from the QD to the cavity. For large detuning the losses cause a slow decay of the exciton population.

5.3 Phonon scattering

5.3.1 Losses, no detuning, phonon scattering

To include phonon scattering in the calculations (see equation 4.22), the strength of exciton-phonon coupling $\lambda_{ee,k}$

$$\lambda_{ee,k} = \sqrt{\frac{k}{2\hat{\rho}c_l}} \int e^{-i\mathbf{k}\,\mathbf{r}} (D_e|\phi_e(\mathbf{r})|^2 - D_h|\phi_h(\mathbf{r})|^2) d^3r \tag{5.5}$$

has to be determined. $\lambda_{ee,k}$ describes a coupling where the exciton deforms the surrounding lattice and a polaron is formed, but no transitions to other QD or cavity states are induced. It depends on electron and hole wave function $\phi_{e,h}(\mathbf{r})$, which is assumed to be Gaussian, and the material parameters of the host semiconductor (see table 5.1).

Table 5.1: Material, dot, and cavity parameters used in our simulations [7]. The phonon parameters are representative for GaAs. For the electron and hole wave functions, we assume Gaussians with a full width of half maximum (FWHM) of L_{lat} and L_z along the lateral and growth direction, respectively. Throughout we use an exciton-cavity coupling strength of 100 μeV and a radiative dot lifetime of 7 ns. The cavity quality factor is $Q = 100000$ unless stated differently.

Parameter	Symbol	Value
mass density	ρ	5.37 g/cm^{-3}
sound velocity	c_ℓ	5110 m/s
deformation potential for electrons	D_e	-14.6 eV
deformation potential for holes	D_h	-4.8 eV
in-plane confinement (FWHM)	L_{lat}	10 nm
confinement in z-direction (FWHM)	L_z	4 nm
radiative decay time of dot	τ_{rad}	7 ns
exciton-cavity coupling	g	100 μeV
cavity photon energy	ω_{cav}	1.3 eV

First, we investigate the influence of phonon scattering for a resonant system (no detuning). In contrast to section 5.2.1 where the minima are always zero, here the minima of the populations of cavity and exciton follow a broad peak for increasing time, as can be seen in figure 5.5. The peak becomes more pronounced when the temperature increases. This peak can be explained by the temperature dependent distribution of phonons in the surrounding medium, which follows the Bose-Einstein-statistics, see equation (4.21). While only a few phonons with low energy can contribute to the scattering process when the temperature is low, phonon scattering becomes an important mechanism for higher temperatures, that influences the respective populations significantly.

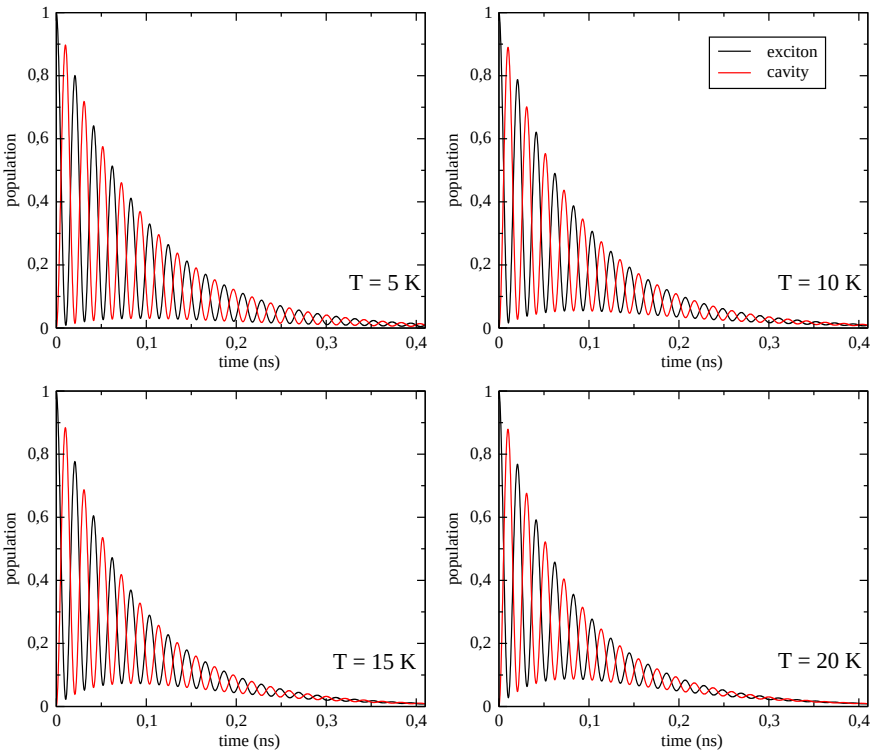

Figure 5.5: Population of the exciton (black lines) and the cavity (red lines) for the resonant case, for increasing temperature $T = 5, 10, 15, 20K$. Losses and phonon scattering are considered.

Cavity feeding rate for increasing temperature

For a better understanding of this phenomenon we investigate the influence of the temperature on the cavity-feeding rate Γ, see equation 4.22. Figure 5.6 shows the cavity feeding rates for the phonon assisted transition from the exciton to the cavity. The peak is rather asymmetric for low temperature $T = 2K$. This can be understood as for such low temperatures few phonons are excited in the host material. Consequently, only positve detuning can be compensated, by means of phonon emission. Increasing the temperature, results in more phonons in the reservoir that can contribute to the scattering. Then also negative detuning can be compensated by phonon absorption. For $T = 20K$ the peak is already rather symmetric, however, still somewhat shifted to positive detuning.

Consequently, we expect different population distributions for positive and negative detuning as is discussed in section 5.3.3 and 5.4.3.

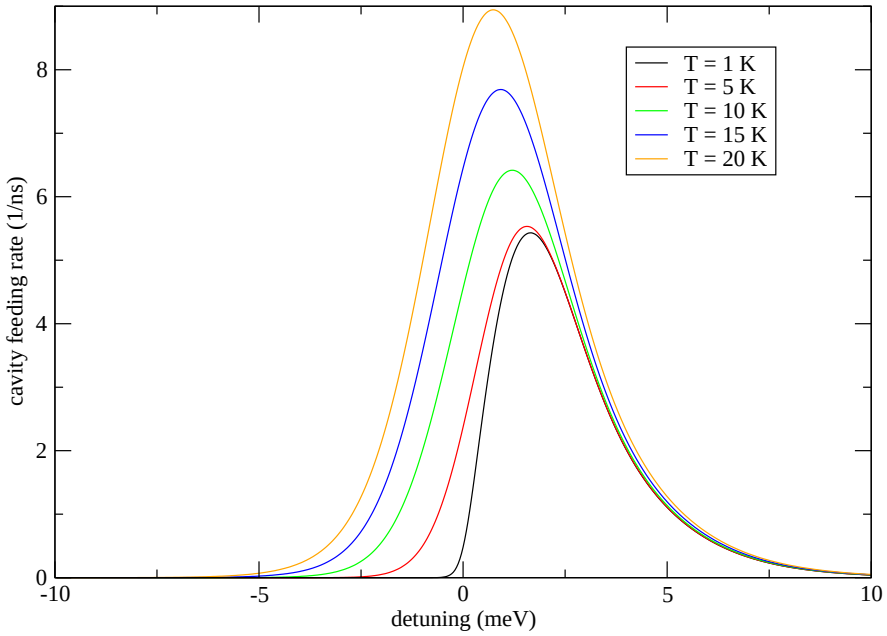

Figure 5.6: Cavity feeding rates for increasing temperature. Losses and phonon scattering are considered.

5.3.2 Losses, detuning, phonon scattering

Now, we are interested in the influence of phonon scattering when the excitonic state and the cavity do not possess the same resonance energy. It can be expected that the energy mismatch (detuning) leads to a weakening of the coupling, as is discussed in sections 5.1.1 and 5.2.2.

First we discuss the influence of phonon scattering on the exciton population. When the QD-cavity system is close to resonance ($\Delta = 0$ eV, $\Delta = 9 \cdot 10^{-5}$ eV) the exciton population does not depend strongly on phonon scattering, as can be seen in figure 5.7. When phonon scattering is considered (red lines) the population decreases faster and the amplitude of the oscillation is smaller. They become more evident, when tuning the system more off resonant ($\Delta = 3 \cdot 10^{-4}$ eV, $\Delta = 9 \cdot 10^{-3}$ eV). For large detuning ($\Delta = 3 \cdot 10^{-3}$ eV) a system without phonon scattering would nearly remain in its initial state (excited exciton), with a low (~ 0.001) oscillation amplitude - almost no coherent coupling is left. Phonon scattering allows a significant population transition to the cavity. The resulting losses in the cavity lead to a strong decay of the exciton population.

Now we turn to the population of the cavity. For low detuning we observe

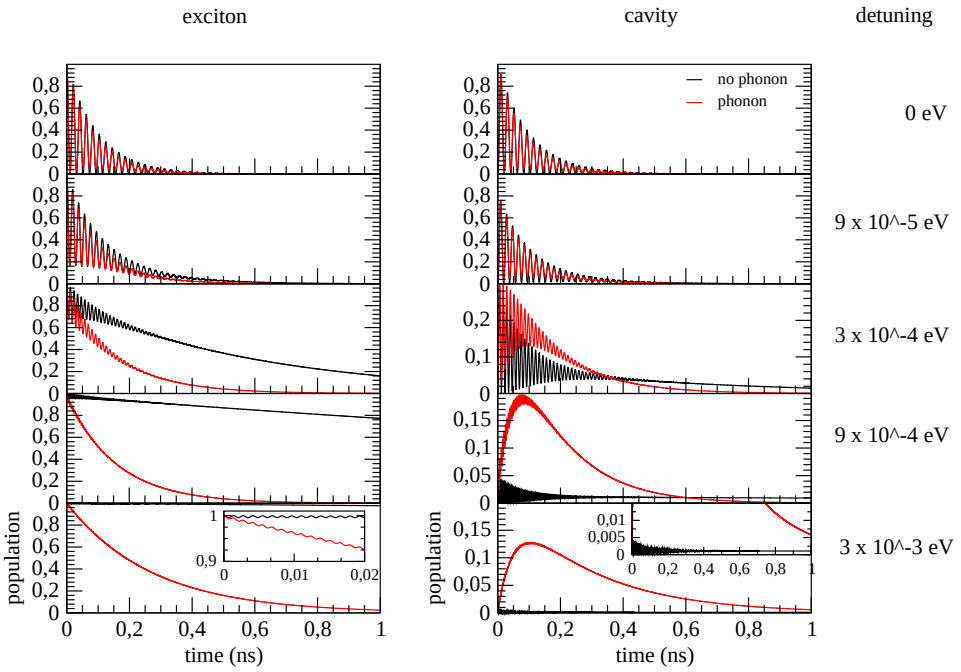

Figure 5.7: Population of exciton and cavity without phonon scattering (black lines) and with phonon scattering (red lines) for T = 10 K.

the same trends as for the exciton population. For increasing detuning phonon scattering leads to a broad population peak (maximum cavity population after $\sim 0.1ns$), which is not evident without phonon scattering. The amplitude of the oscillation of the cavity population decreases with increasing detuning. For large detuning a strong cavity peak is left with a very low oscillation amplitude.

This effect supports the theory of phonon assisted exciton-cavity transition and allow for an explanation of an experimentally detected cavity peak for a system that is far off resonant [5, 8].

5.3.3 Losses, positive / negative detuning, phonon scattering

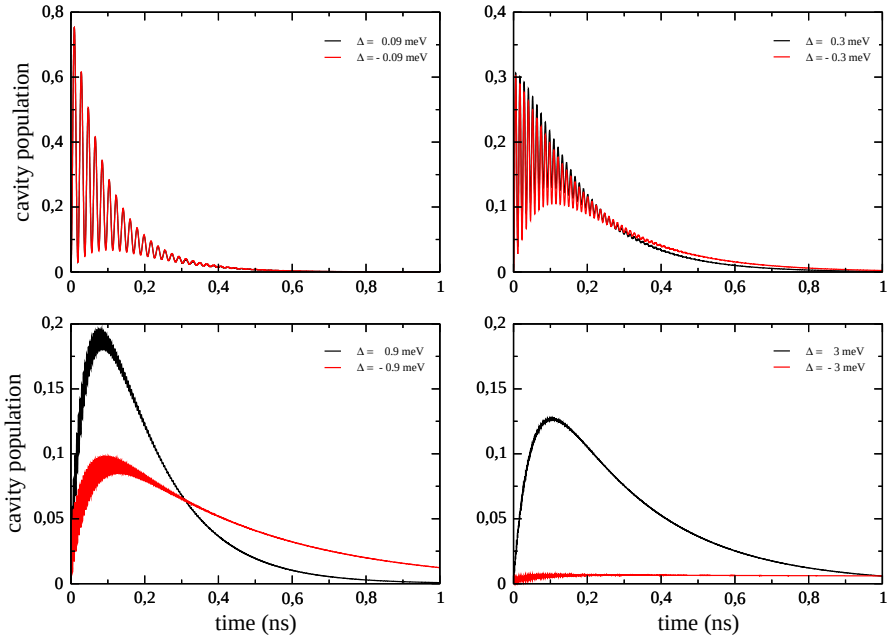

Figure 5.8: Cavity population with phonon assisted cavity feeding for positive and negative detuning; T = 10 K.

We expect that the time dependent populations are not identical for positive ($E_{qd} > \hbar\omega_{cav}$) and negative ($E_{qd} < \hbar\omega_{cav}$) detuning, because the scattering processes are different and the cavity feeding rate is not symmetric, as discussed for figure 5.6. For very low detuning values ($\Delta = \pm 0.09\,meV$) we can hardly see a difference between positive and negative detuning in figure 5.8. But when detuning increases, we observe pronounced differences. For $\Delta = 0.9\,meV$ we find a cavity peak that is twice as high for positive detuning, but it decays faster. For $\Delta = 3\,meV$ we find a cavity peak with a maximum value of 0.12 at $t = 0.1\,ns$ for positive detuning while the cavity population is significantly lower for negative detuning.

For higher temperatures these differences should be less pronounced.

5.4 Pumped system

5.4.1 No detuning

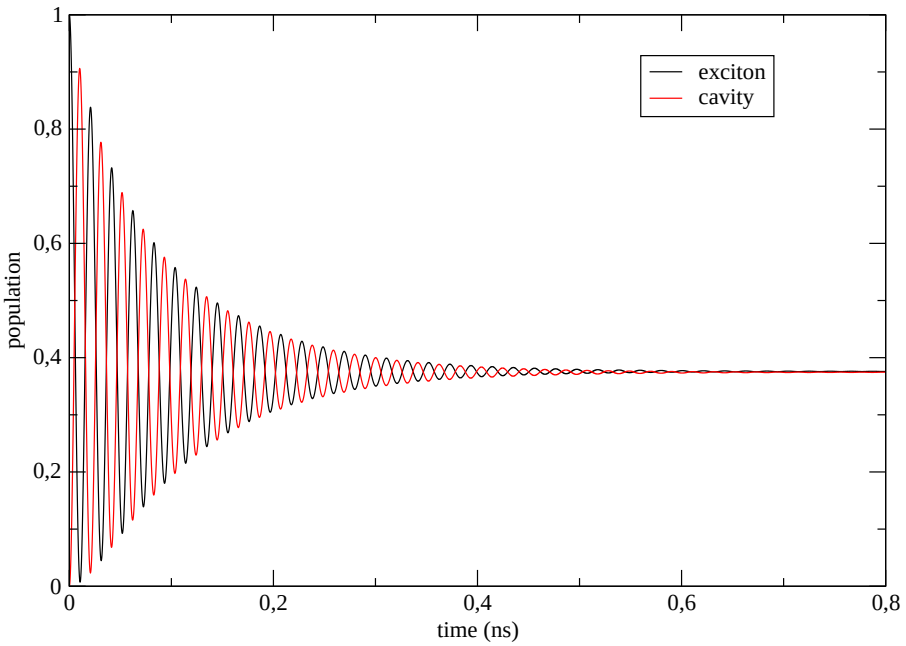

Figure 5.9: Population of the exciton (black lines) and the cavity (red lines). Pumping, losses but no phonon scattering are considered.

Now, we are interested in a pumped QD-cavity-system, i.e., the exciton is frequently excited, for example with a laser. First we discuss a resonant system (no detuning). As already discussed in sections 5.2.1 and 5.3.1 the populations of QD and cavity decay exponetially and become zero due to losses, when a single exciton excitation is considered.

Pumping the system strong enough (pumping rate > loss) the system "equlibrium". The populations of QD and cavity converge to constant values. For the resonant case QD and cavity converge almost to the same value as can be seen in figure 5.9. The "Equilibrium" state is assumed after $2\,ns$.

5.4.2 Detuning

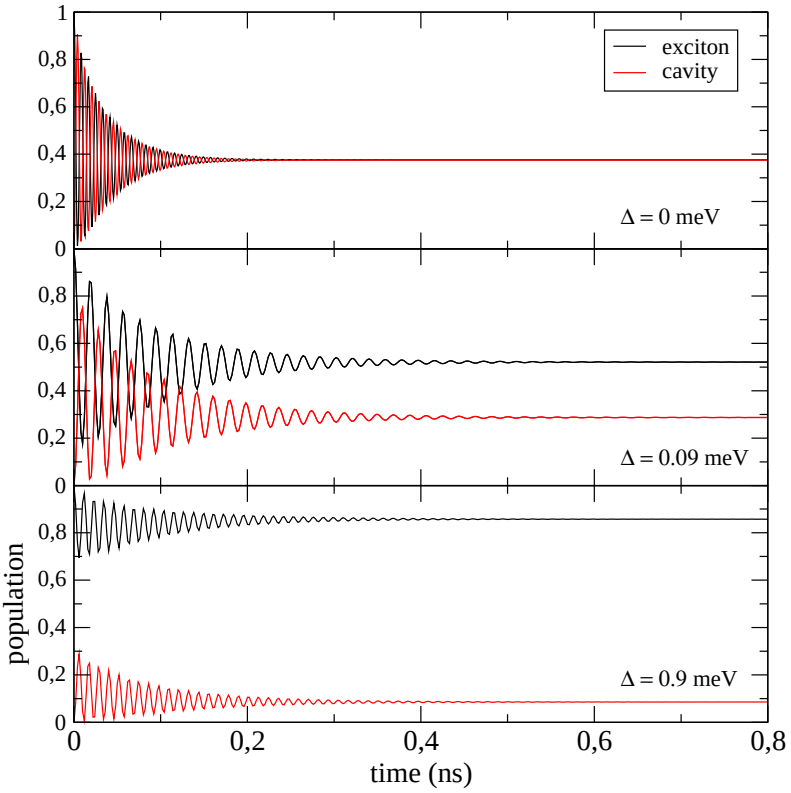

Figure 5.10: Population of the exciton and the cavity for a resonant and for detuned QD-cavity-systems. Losses and pumping are considered. No phonon scattering is considered.

When the QD is detuned with respect to the cavity the population transfer from the QD to the cavity is hindered. In steady state this results in a lower cavity population and a higher QD population, as can be seen in figure 5.10. This behavior is equivalent to the trends discussed in sections 5.1.1 and 5.2.2.

5.4.3 Positive / negative detuning, phonon scattering

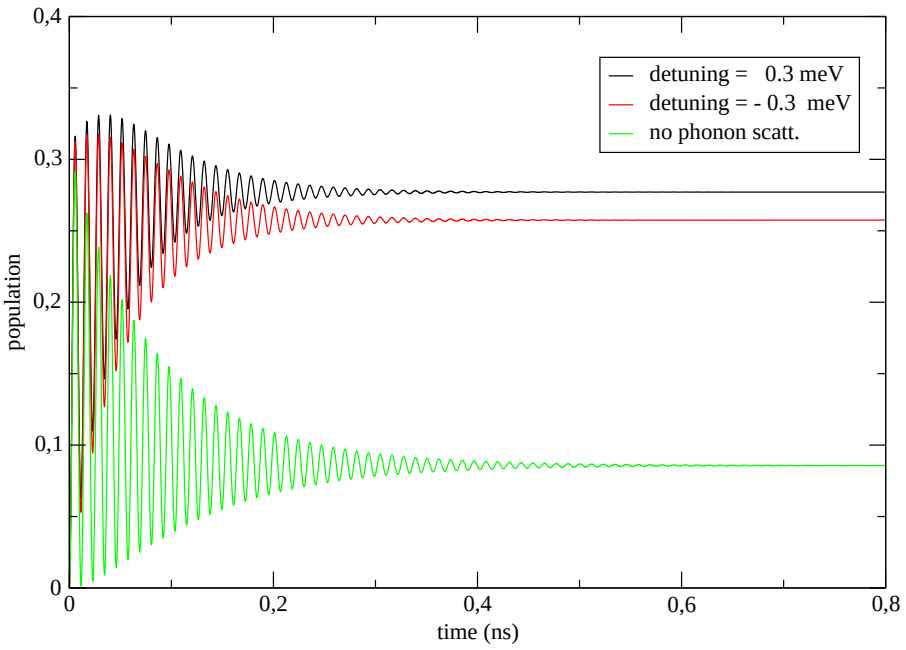

Figure 5.11: Population of the cavity for positive and negative detuning $\Delta = \pm 0.3meV$ for a driven system. For comparison, we add the cavity population for a system without phonon assisted cavity feeding and detuning $\Delta = \pm 0.3meV$. T = 20 K.

Now we are interested in the influence of phonon scattering on the cavity population in steady state. Again we observe an increased cavity population due to phonon assisted cavity feeding, as can be seen in figure 5.11. Compareable to section 5.3.3 the exact value in steady state is different for positive and negative detuning, as can be expected from figure 5.6.

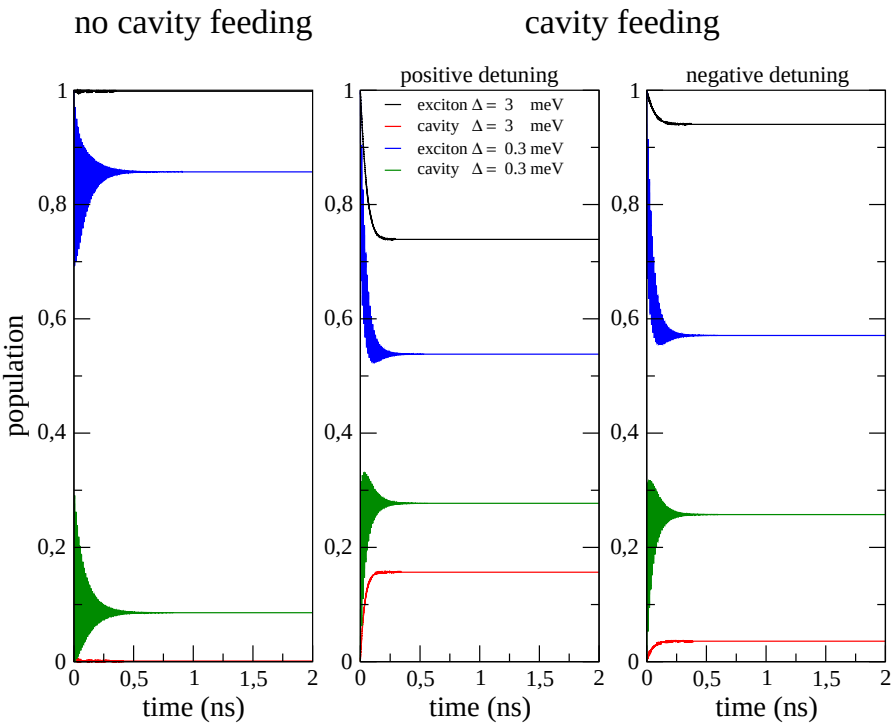

Figure 5.12: Population of the exciton and the cavity without cavity feeding (phonon scattering) and with cavity feeding and positive ($\Delta = 0.3\,meV, 3\,meV$) or negative detuning ($\Delta = -0.3\,meV, -3\,meV$). Pumping and losses are considered. $T = 10\,K$.

The influence of phonon scattering is summarized for two different detuning values in figure 5.12.

5.4.4 Temperature dependence

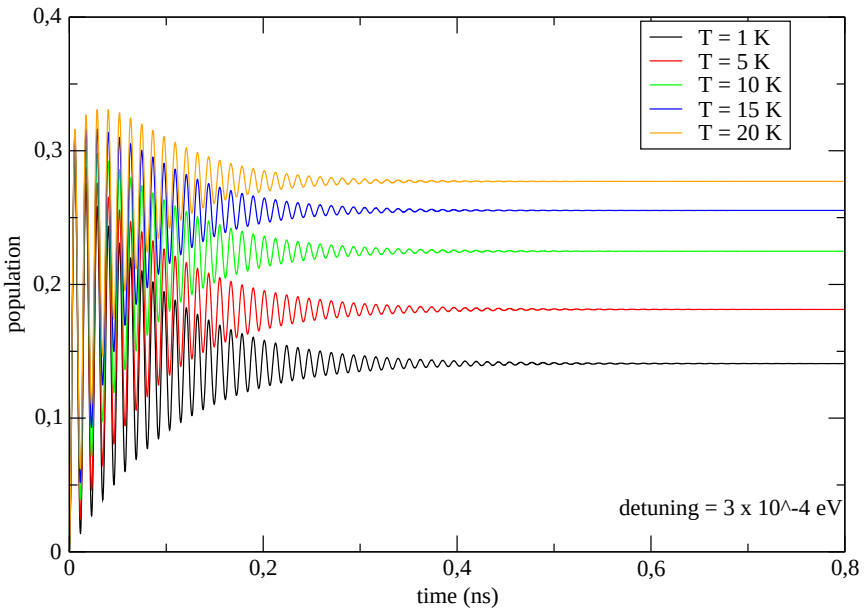

Figure 5.13: Cavity population for a driven system for different temperatures T and a fixed detuning $\Delta = 0.3meV$. The strength of pumping is $1.5 \times \kappa$.

The population of the cavity for a driven system for different temperatures $T = 1$ to $20\,K$ is shown in figure 5.13. Increasing the temperature leads to a higher value of the cavity population in steady state. As already discussed before, this is due to a higher population of phonons, compare section 5.3.1 and figure 5.6.

5.4.5 Steady state, varying detuning

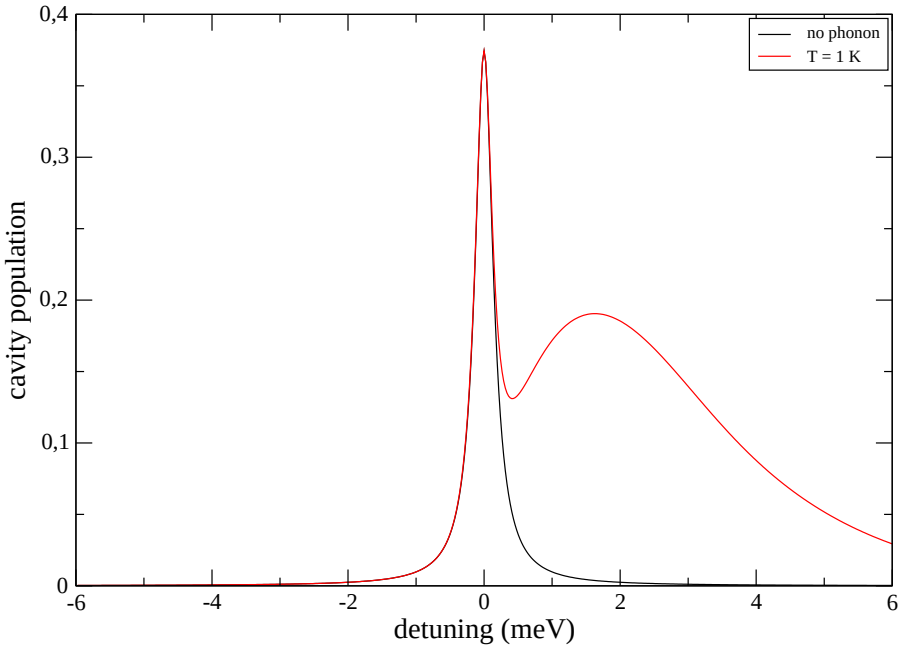

Figure 5.14: Cavity population after $2ns$ (steady state) without and with (T = 1 K) phonon scattering.

Now, we are interested in the steady state values of the cavity population for varied detuning. When phonon scattering is not considered we find a symmetric population peak with a maximum for $\Delta = 0\,eV$, shown in figure 5.14. When phonon scattering is considered a second broad peak can be observed for positive detuning $\Delta > 0\,eV$. This second peak can be explained by the fact that phonon scattering is basically restricted to phonon emission for low temperatures (see section 5.3.1), thus only positive detuning can be compensated. The second peak is more pronounced for low temperatures ($\sim 1K$) as can be seen in figure 5.15. Increasing the temperature leads to a more symmetric and stronger phonon scattering rate (see figure 5.6). Then the second peak shifts towards the resonance peak of the steady state cavity population, being thus less pronounced. For $T = 20\,K$ only a shoulder is left on the $\Delta > 0\,eV$ side. In addition, the population curve is broadend for higher temperatures. Consequently, significant cavity populations can be obtained for large detuning (off resonance). This effect is called *phonon assisted cavity feeding*.

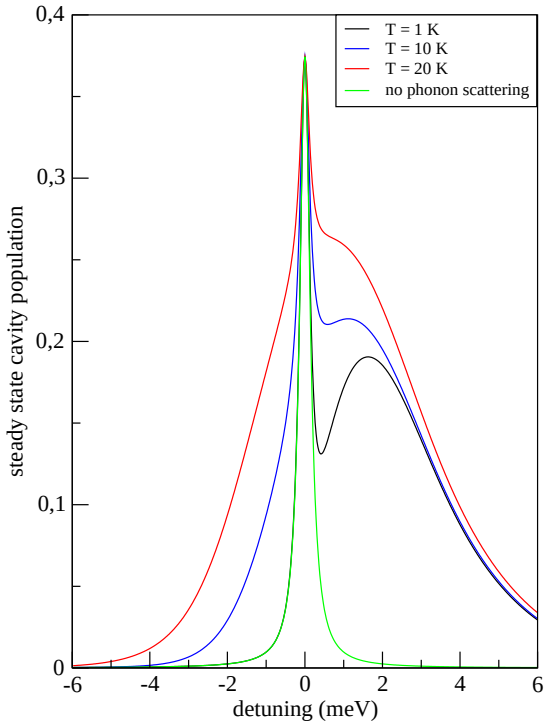

Figure 5.15: Equilibrium values -after $2ns$- for the cavity population for varied detuning for different temperatures. (a) to take backscattering into account (b) just scattering from exciton to cavity. As can be seen the plots of graph (b) are broader.

Bibliography

[1] H. P. Breuer and F. Petruccione. *The Theory of Open Quantum Systems.* Oxford, 2003.

[2] S.M. Dutra. *Cavity Quantum Electrodynamics.* Wiley series in lasers and applications. John Wiley & Sons, Inc., 2005.

[3] J. M. Fink et al. Climbing the jaynes-cummings ladder and observing its $\sqrt{n}$ nonlinearity in a cavity qed system. *Nature*, 454:315–318, 2008.

[4] H. Friedrich. *Theoretical Atomic Physics.* Springer, 1991.

[5] K. Hennessy et al. Quantum nature of a strongly coupled single quantum dot-cavity system. *Nature*, 445(896), 2007.

[6] U. Hohenester. *Optical properties of Semiconductor Nanostructures: Decoherence versus Quantum Control.*

[7] U. Hohenester. Cavity quantum electrodynamics with semiconductor quantum dots: The role of phonon-assisted cavity feeding. *arXiv:0912.5181v1*, 2009.

[8] U. Hohenester et al. Phonon-assisted transition from quantum dot excitons to cavity photons. *Physical Review B*, 80(201311(R)), 2009.

[9] G. Jaritz. Coupling between quantum dot excitons and microcavity photons. Master's thesis, University of Graz, 2009.

[10] M. Kronenwett. Photon correlations in two-mode cavity quantum electrodynamics. Master's thesis, University of Auckland, 2007.

[11] M. Winger. *Mesoscopic Cavity QED with a Single Quantum Dot.* PhD thesis, ETH Zürich, 2009.